ACCOUNTS
of chemical research

Photophysical Probes for Multiple-Redox and Multiple-Excited-State Interactions in Molecular Aggregates

MARYE ANNE FOX

Department of Chemistry and Biochemistry, University of California, San Diego,
9500 Gilman Road, La Jolla, California 92305, United States

RECEIVED ON JANUARY 3, 2012

CONSPECTUS

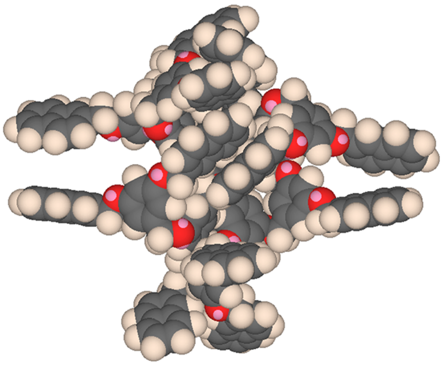

Photosynthesis takes place through a highly efficient series of energy, electron, and proton transfers initiated by absorption of one or more photons within the visible region of the solar spectrum. Because of the presence of multiple chromophores needed for effective light harvesting, extinction coefficients must be very high. The absorbing multiunit array is held within a rigidly arranged structure that facilitates each electron hop.

A fully artificial, yet biomimetic, alternative to photosynthesis that produces fuels directly and efficiently from sunlight and simple low molecular weight molecules would change the world. Achieving this goal requires a detailed understanding of the mechanisms of the key steps of the complex chemical and photochemical processes taking place in natural photosynthesis. One of these mechanisms relies on light harvesting to initiate multiple-step sequences to obtain combustible molecules suitable for burning. In particular, we are devising and testing photophysical models with characteristics that facilitate multiple electron transfers within a single aggregate and are directly relevant to light harvesting. We focus on structural features that promote photoinduced electron transfer at high dye densities, placed for optimal solar utilization and catalysis.

The reaction producing oxygen is further complicated by the need for four electrons to complete the sequence, even though the first initiation step is presumably absorption of a single photon. Therefore we explore steps that accumulate charge or have the potential to do so. We also emphasize the synthesis of model systems that probe the complexity of individual steps.

This Account examines the factors that influence the efficiency of electron redistribution in multiple-dye, multiple-excited-state, and multiple-redox equivalent arrays. Such knowledge will allow us to optimize the efficiency of electron migration and may contribute to a better understanding of multiple-equivalent light harvesting events by which photosynthetic energy storage takes place.

I. Natural Photosynthesis

Natural photosynthesis is one of the most complex of all processes on earth. It is also one of the most important, representing a vital component regulating the balance among atmospheric gases. Although it involves a complex set of quite different reactions, photosynthesis is initiated by a light-driven sequence that, when completed, supports life on earth as we know it. This is accomplished by effecting the chemical reduction of carbon dioxide to sugars and the oxidation of water to oxygen (O_2). It is therefore responsible also for regulation of our oxygen-based atmosphere. Life on earth is fully dependent on natural photosynthesis, which includes as well respiration and the production of food, fiber, and fuel. These, in turn, are used in oxidative metabolism in plants, animals, and humans.

Both natural and artificial photosynthesis are initiated by the absorption of light. The key steps of photosynthesis must, of necessity, involve multiple excited states, direct formation of which is forbidden electronically in simple models. It also requires a catalytically active site that can accumulate multiple redox charges. We cannot hope effectively to model natural photosynthesis without investigating how the local environment of a photochemical reaction center in an artificial model is affected by aggregation effects.[1−8]

Biomass and fossil fuels have been used over recorded history as primary sources for energy released for combustion.

www.pubs.acs.org/accounts
10.1021/ar3000037

They are obtained by decay of organic molecules over geological time scales derived directly or indirectly from photosynthesis. But direct combustion of fossil fuels also releases large quantities of carbon dioxide, a greenhouse gas whose presence in the atmosphere contributes to global warming and problematic climate change.

Most alternate energy proposals involving biofuels, liquids obtained from plant sources such as corn, lignin, grasses, or algae, employ the products of photosynthesis as a source of stored energy, releasing CO_2 upon combustion. That is, biofuel production takes place via enzymatic degradation of other products of photosynthesis, through pathways that also release CO_2 upon combustion. The search for completely artificial pathways for energy production, likely employing evolution-optimized principles for multiple steps, is a highly worthy scientific goal.

II. Artificial Photosynthesis

Developing a fully artificial, yet biomimetic, alternative to photosynthesis to produce fuels directly and efficiently from sunlight and simple low molecular weight molecules, carbon dioxide and water, for example, would be a world-changing accomplishment. This goal can be reached, however, only if we understand in detail the mechanisms of the key steps of the complex chemical and photochemical processes taking place in natural photosynthesis.

One of these uses light harvesting to initiate multiple-step sequences to obtain, eventually, combustible molecules suitable to be burned, that is, release the energy of stored chemicals in conventional incinerators. The second uses solid state solar cells as immediate providers of energy demands for usage as electrical current or as stored in a charged battery.

In particular, we seek to devise and test appropriate photophysical models that define characteristics that facilitate multiple electron transfers within a single aggregate[12,13] and have direct relevance to light harvesting. We focus on those structural features that describe photoinduced electron transfer[9−13] at high dye densities, placed for optimal solar utilization and catalysis. In the available space, we can only bring along a representative discussion of catalysis or photocatalysis in self-assembled monolayers (SAM),[14−23] in reactive shell−core clusters (SCC),[24−28] in functional polymers,[29−36] and in dendrimers.[37−47] These families are highlighted because each class bears structural features that could possibly accommodate multiple charges when properly functionalized. It is also important that we consider how physical dispersal of dyes in those arrays affects the excited states of fully loaded aggregates, how directionality toward a target must be included in molecular design, and what competing paths[48−53] influence the long-term stability of the whole array. We also take a quick overview of applicable devices[54−59] that are dependent on high density chromophores and efficient photoinduced electron transfer. The synthetic designs in which the reaction centers are imbedded can then be compared with the results when the reaction centers are imbedded in sol gels.

The compounds being studied all possess either an electron donor and an acceptor, a site to complex with a stable metal ion, or a sensitizer capable of efficient energy transfer. Intersystem crossing is enhanced by covalent bonding onto a scaffold of a different structural type. For example, very rigid packing of the terminal group takes place in a SAM, compared with SCCs or dendrimers. As a result, we expect to see variance with the scaffold and with conformations in the connecting tether that range from rigid to highly flexible.

Eventually such molecules may find use in high efficiency artificial solar cells, although the requirement for extraordinarily high turnover at each step of the catalytic sequence mitigates against practical utilization of the most highly absorptive organic compounds. Almost all have competing photochemical reaction pathways, making long-term stability a serious limitation.

Typically a solar cell either directly converts or stores high energy molecules in a dark battery in which the equilibrium position is shifted, favoring reduction by solar illumination. Of special significance are the effects of aggregation and conformational flexibility on the efficiency with which energy is stored via excited state reactions that take place on the organizing surface. The scaffold influences the relative positions of the chromophores against homogeneous dispersions. This range of conformational equilibration thus enables variance in structural rigidity in each of the organized arrays considered below.

The efficient use of light in photosynthesis is accomplished through energy migration and ultimately through a plant's ability to collect multiple photons within its light harvesting complex. If we understood in detail how these assemblies act as photoresponsive multichromophoric arrays, we could, in principle, greatly improve our approaches to an efficient biomimetic solar conversion device. We would also learn fundamental properties likely to be the most important in achieving practical energy conversion. Thus, the characteristics being studied as models include (1) broad and strong spectral absorption in the visible region of

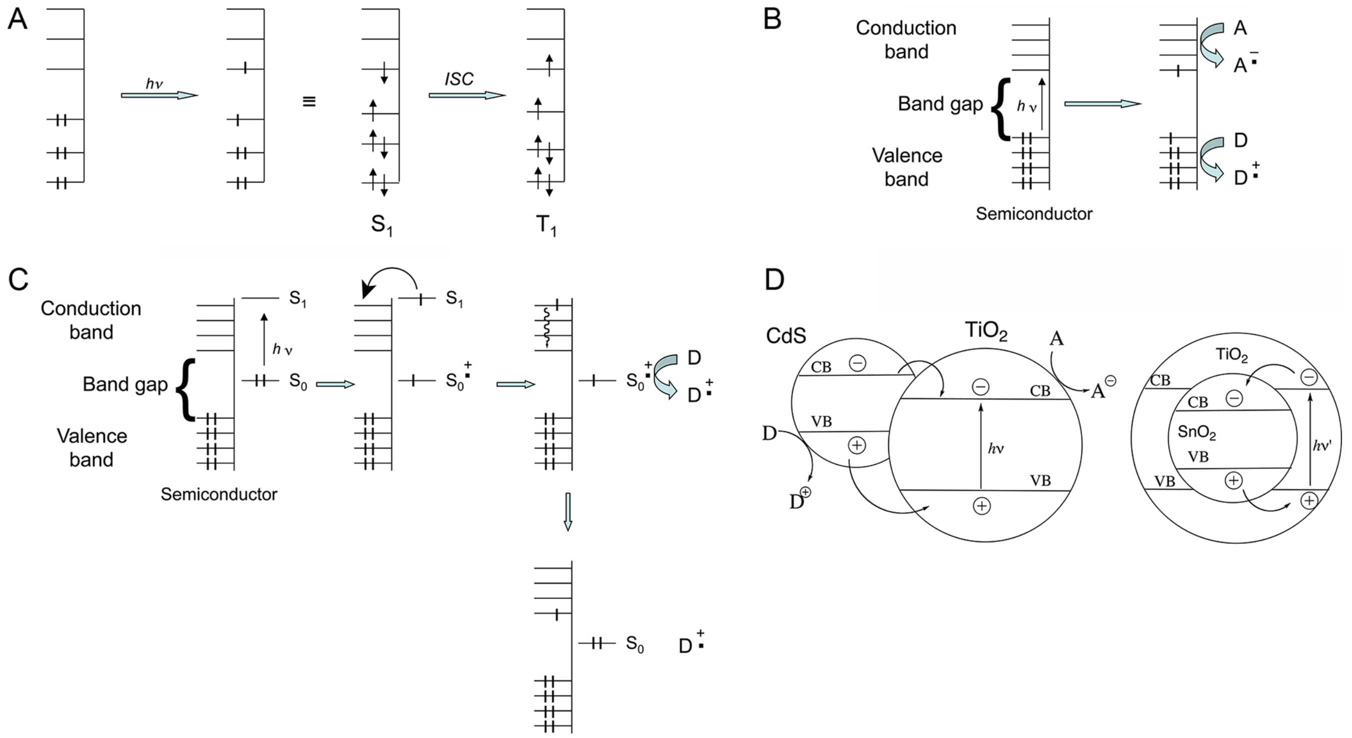

FIGURE 1. Reaction systems initiated by photon absorption: (A) photochemistry; (B) photoelectrochemistry; (C) photosensitization; (D) multiple electron hops on composite semiconductor particles.

the electromagnetic spectrum, (2) the presence of multiple dyes or pigments, (3) constraint to designated three-dimensional sites, for example, in H or J aggregates, and (4) binding onto an inexpensive scaffold. Thus, identifying synthetically accessible analogs of light harvesting arrays would be of inestimable value in understanding the complexities of photosynthesis.

III. High Density Dye Aggregation

For several decades, highly sophisticated instrumentation has been used to explore the similarities and differences among densely packed light harvesting arrays in natural photosynthesis and those present at multiple reaction centers in aggregated dyes and catalysts. Although the multiredox center often complicates observed reactivity, the very complexity of such reactions taking place at interfaces allows for discovery of new and exciting chemical pathways.

Many light harvesting arrays have been used as preferred materials to study the desired complexity, while simultaneously retaining predictable local clustering. The ready availability of nanoparticles as precisely sized supports for catalysis and for photocatalysis has eased this process appreciably. We can now study much more readily the photophysical, photochemical, and photocatalytic properties of clusters and surfaces of nanomaterials and biological samples on a fixed support. These include, among others, organic and inorganic sol–gels, functionalized shell–core dendrimers, polymers of varying chemical type and structural complexity, porphyrinic liquid crystalline clusters that stack as liquid mesophases self-assembled monolayers on atomically flat or regular spherical supports, shell–core dendrimers, arrays in which multiple dyes saturate transmission of incident light absorption, and biological scaffolds.

These supports bind specific chromophores in precisely arranged geometric structures that permit or inhibit noncovalent association of the dyes. We have been particularly interested in scaffolds that develop directionality to enhance spatial migration of electrons, attached groups constituting a gradient for energy or electron transfer. It is our hope to test exciton migration through tightly packed clusters of highly localized dyes or catalysts for dendrimers in solution and on polymer supports.

Analogous commercialized clusters provide insight into nonbiological models that are multichromophoric but are far from being well understood or optimized. For example, molecular logic devices, tagging of specific cells by light-sensitive biosensors, columnar stacking, new reversible chemical switches, and all-inorganic solar cells all depend on clustering for acceptable catalytic turnover. Discussing even this abbreviated list, however, would exceed the format of an Account. Instead, we focus on multiple electron hops, including brief discussions of organic and inorganic dendrimers, SCCs, and SAMs and their optical properties.

In particular, in this Account, we devise and test appropriate photophysical models that define characteristics that facilitate multiple electron transfers within a single aggregate. We focus on those structural features that describe electron transfer in self-assembled monolayers (SAM), in shell–core clusters (SCCs), and in dendrimers. These families are highlighted because each class bears structural features that could possibly accommodate multiple charge catalysis when properly functionalized. It is also imperative that we consider how physical dispersal of dyes in those arrays affects the excited states of fully loaded aggregates.

IV. Photoinduced Electron Transfer (PET) and Photochemistry

Any discussion of the photophysical properties of multiunit events must begin with a description of the interdependence of structure and reactivity in light-driven orbital population changes, Figure 1a. Several activation routes are generally followed when a molecule is exposed to ultraviolet or visible irradiation. These pathways include (1) photochemical excitation as a route to bond making and breaking, (2) direct PET, producing an associated ion pair in homogeneous solution, (3) photocatalysis and photoelectrochemistry, most frequently forming oxidative redox products in aerated solutions, or (4) dye-sensitization at monolayer or multilayer coverage.

Shown in eq 1 is the result of photoinduced electron transfer, producing an oxidation–reduction pair. This transformation can take place either in solution or while associated with a solid support. If the solid support is a semiconductor that strongly absorbs incident light, it could serve as a photocatalyst, capable of producing a surface-bound electron–hole pair, which can favor secondary dark reactions.

Interfacial electron transfers complete the oxidative sequence. If the solid surface is a conductive metal, the continuum of states largely dissipates stored energy as heat, facilitating fast recombination of the electron–hole pair. Flash photolysis produces an excited state whose decay to the ground state is very rapid.

$$D + A \rightarrow D + A \qquad (1)$$

a. Direct Photolysis in Solution and on Surfaces. Before absorption of a photon, an electron-rich donor D equilibrates with an electron-poor acceptor A, having adsorbed to the solid of interest. The energy difference in homogeneous solution between the highest- and lowest-lying occupied orbitals is sufficient to form the initial excited state as a singlet, that is, one in which the spins of all electrons are paired. If one of the paired spins flips, a triplet state is formed.

Upon photoexcitation of the semiconductor, however, a pair of ions is generated, with D becoming a cation and A becoming an anion, eq 1. This separation of charge in the ion pair constitutes net energy being stored as electrochemical potential. Charge separation also permits a physical migration of oppositely charged ions toward each other, allowing charge neutralization, for example, in the complex biological system in which the probe molecule is included on the reaction scaffold. How strongly the ions interact will depend on the flexibility of the intervening tether (or lack thereof).

Superexchange, the mixing of higher lying states into the initial singlet or triplet excited states, may enhance the separation of charge. The extent to which the geometry of the ion pair is altered by PET causes a reorganization, which is costly energetically and will affect the observed lifetime of the ion pair.

Similar shifts are also observed when the contact ion pair is strongly solvated. Each factor also influences the rate of back electron transfer, attaining charge recombination and allowing the ion pair, with no net conversion, to relax back to the ground state. As a consequence of the absorption of a photon, charge separation takes place, with the site that was previously electron-rich actually becoming a cation, and the converse happening to the acceptor, that is, the initially electron-poor species becomes formally an anion. An oversimplified orbital description of the fate of a neutral molecule adsorbed on a semiconductor particle suspended in aerated solution upon exposure to visible or ultraviolet irradiation (photochemistry) is shown in Figure 1b.

b. Photoelectrochemistry and Photocatalysis. PET takes a similar course when D and A are adsorbed onto a neighboring surface site on a semiconductor particle or film. This process, when initiated by absorption by the solid support, called photoelectrochemistry, is illustrated in Figure 1b. Under optimal conditions, a semiconductor surface, modified by adsorption of a specified reactant as a gas or liquid, is irradiated with light having an energy greater than the band gap, that is, the energy difference between the valence and conduction band edges. This irradiation produces an electron–hole pair at the surface of the metal oxide scaffold, created just at or above the highly oxidative valence band edge, which then accepts an electron from the adsorbate D.

The freed electron is trapped at the energy of the conduction band edge. Thus, interfacial ET, that is, photocatalysis on an irradiated semiconductor surface, ultimately produces the same ion pair as in Figure 1a.

The energy of the photoinduced ion pair formation is always less than or equal to the separation between the valence and conduction band edges, and this value thus serves as a maximum for any contemplated redox conversion. Because the energy difference is large for metal oxides, ultraviolet light must be used to start the photoelectrochemical sequence, with a typical incident wavelength of about 410 nm or less. Simultaneous bonding of O_2 and the substrate onto the metal oxide surface opens a route for subsequent migration of the electron and hole along the activated surface, Figure 1b. Trapping of the migrating electron by coadsorbed oxygen disrupts electron–hole pair binding and activates the adsorbed reactant to catalytic oxidation via interfacial electron trapping.

c. Photosensitization. In contrast, photosensitization is a process by which a highly colored absorptive dye is excited but transfers its singlet or triplet energy to another molecule before the excited absorber can itself react, Figure 1c. (The terms "sensitizer" and "photosensitizer" are used interchangeably, indicating initial photoexcitation energy is used to produce a low energy singlet or triplet excited state, Figure 1a, rather than by the support or reactant itself, as in Figure 1, panel a or b). That is, in photosensitization, the adsorbate, not the metal oxide support, takes on the incident photon, directly producing the singlet state encountered in Figure 1a.

When the sensitizer is dissolved in solution or adsorbed on a suspended semiconductor particle, however, an excited state of the sensitizer (the same as ultimately produced in Figure 1b) injects an electron into the adsorbate. The result is the same adsorbed redox ion pair, but without direct photoexcitation. This same pair would have been formed had the adsorbate been subjected to band gap irradiation via photoelectrochemistry, that is, through the process illustrated as Figure 1, panels c and d.

d. Multiple Electron Hops in Composite Semiconductors. Finally in Figure 1d is shown how each process is adapted to multiple hops and, by inference, to other multiple events. Each composite can be considered a perturbation of the photoelectrochemical approach attained via multiple electron hops on composite particles, Figure 1d. Structurally, two types of semiconductor particles are prepared by one of two routes: either (a) from the core preformed before mixing with the outside shell layer being deposited in a second step or (b) by jointly mixing the two substrates, forming patches of one particle on the other, as shown by the left diagram. Best photoefficiency, that is, the highest fraction of incident photons that ultimately appear as stored energy, is attained when the chosen excitation wavelength matches the absorption or action spectrum of the two photocatalysts. Thus, judicious choice of the specific synthetic method allows for differentiation of two-component (or more) particles, both (or all) of which possess a large internal macroscopic dipole.

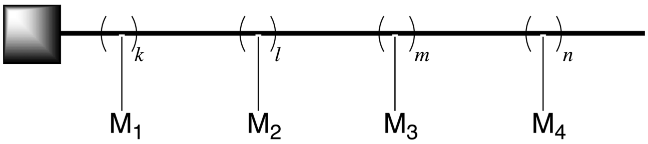

FIGURE 2. Gradients for electron or energy transfer.

V. Directional Electron Transfer

The clear objective of photoinduced electron–hole pair formation in photocatalysis is the long-term separation of charges. This produces intermediates sufficiently long-lived to permit chemical conversion and storage. The high redox potentials of the ion pair are used chemically in a second step to give the desired redox products. The further the opposite charges can be separated physically, the more efficient will be the net oxidation or reduction reaction, because distance inhibits recombination.

In this route, the charge-separated electron and hole, produced by any of the photoinitiated routes described above, are further activated toward making multiple hops over even longer distances than discussed above. It has also has been demonstrated in donor–acceptor 1–acceptor 2 triads, so long as there exists a definable energy gap driving unidirectional migration of the charged ion pair components. If the mediators bound to (or constituting) the support are energetically ordered, directional transfer can take place.

Figure 2 illustrates this concept. When the series $1 > 2 > 3 > 4$ represents a series of declining oxidation potentials, the trapped charge will move preferentially down a defined energy gradient to a target, thus chemically differentiating one end from the other. By anchoring one end of the bifunctional linker to the metal or semiconductor support and binding the other end to a photophysical probe molecule, we can observe charge migration, mostly to the left as written here, accumulating multiple charges at the trap. Well-developed coupling routes have been used to achieve nearly complete monolayer attachment, and the reverse order of the series $1 > 2 > 3 > 4$ generates the oppositely dispersed array. In the latter series, the macroscopic dipole is

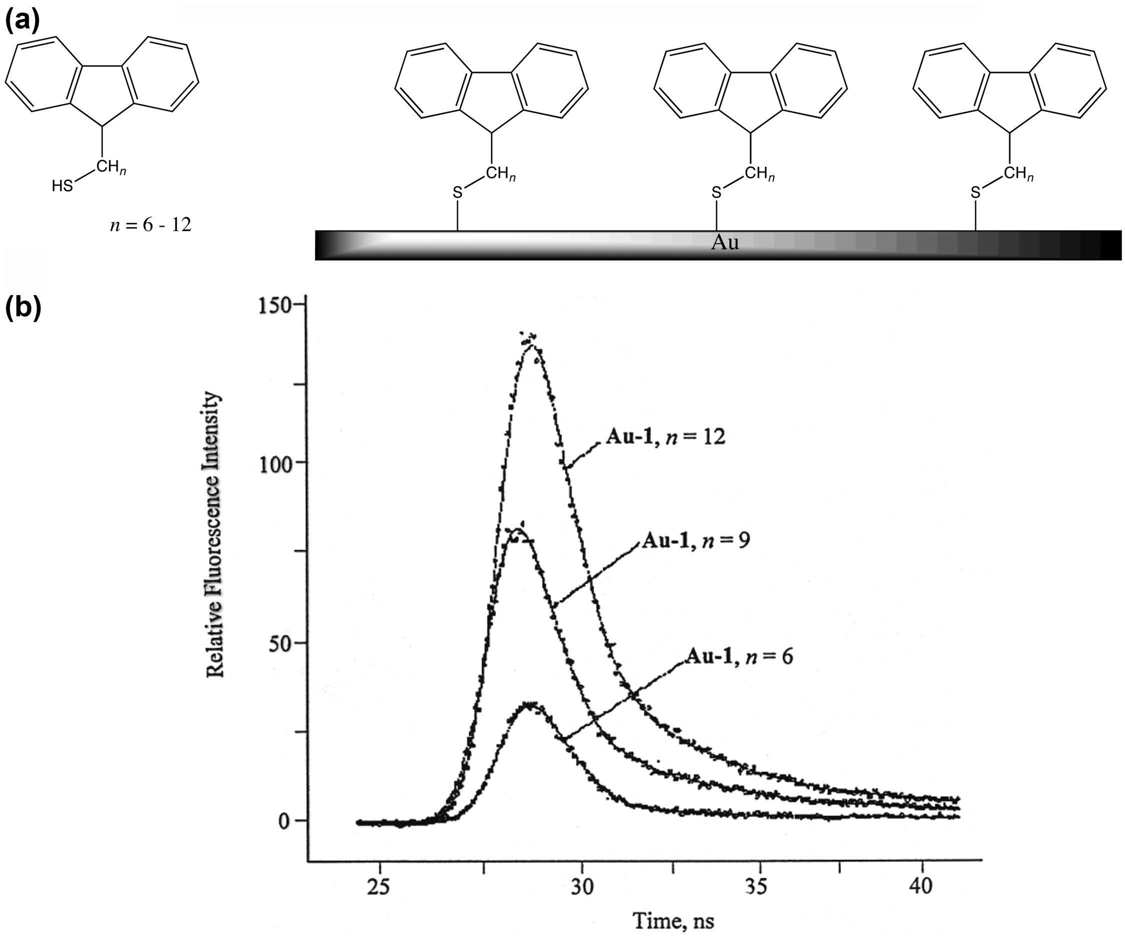

FIGURE 3. (a) Chain-length dependent charge transfer; (b) chain-length dependent fluorescence.

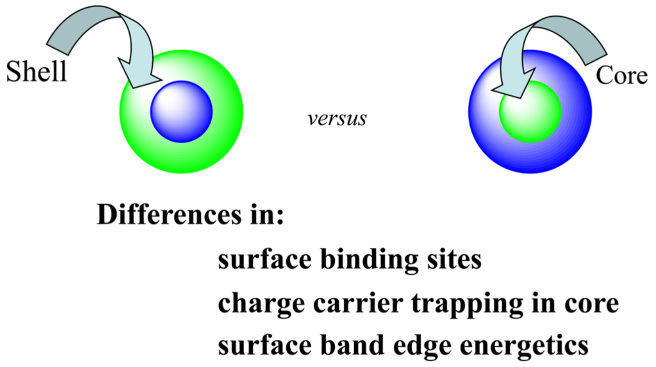

FIGURE 4. Shell–Core Clusters.

completely inverted from the first arrangement mentioned above.

In principle, it ought to be possible to anticipate at most one charged ion pair per absorbed photon produced during intense irradiation of multiply substituted tethers. If the migration target is a cathode/anode pair imbedded within an electrochemical cell and if the irradiation penetrates the cell wall, electrochemical storage of solar energy will have been attained. These cells have been reduced to practice for highly porous polymers derived from a wide variety of monomers. Among this group is a plethora of ion-exchange resins whose value to electrochemistry has been recognized over many years. Migration of charge, when spatially and directionally controlled, is also a key component of quantum computing. In the next section, we provide examples of how aggregation influences chemical catalysis and excited state interactions in multiply dye-loaded materials.

VI. Polymeric Aggregates

Polymer-induced energetic ordering is accomplished by binding energetically ordered blocks of functionalized dyes of polymerizable A–B monomers, and host–guest aggregated arrays can also be attained by binding small molecules covalently to a pre-existing polymer. Members of both of these families represent new opportunities for observing biomimetic directional and long-lived ion pairs. Typically, such polymers are conformationally loose, and the conversion of one three-dimensional structure to another is

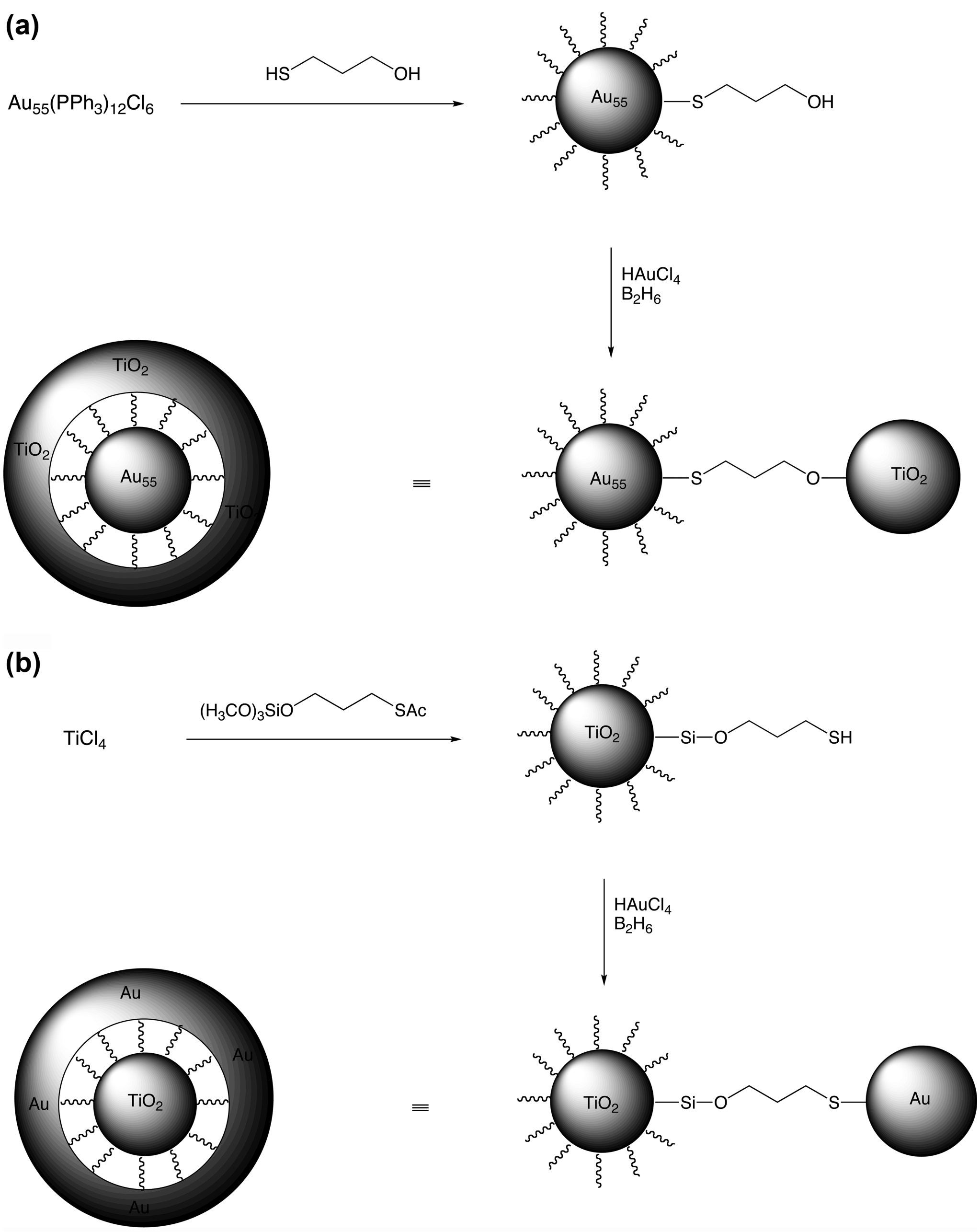

FIGURE 5. (a) Semiconductor-capped metal nanoparticle; (b) metal-capped semiconductor nanoparticle.

relatively easy. Although this field is blossoming, it is also far too broad to be covered in an Account and will be discussed elsewhere.

However, attaching dyes in regular fashion along a polymeric chain generates a species that permits multiple-photon or -electron events to take place through a space controlled by conformational motion.

VII. Self-Assembled Monolayers

Self-assembled monolayers are tightly packed arrays in which an adsorbate is end-functionalized, leading to a well-defined conformation for the attached groups and or the intervening chains bound to a surface. Only minimal movement can take place across the monolayer surface because the groups of interest are chemically bound, via a laterally interactive insulated linker, usually 6–16 linked carbon atoms, present as a saturated chain and tilted at an angle to ensure maximal tight packing.

As a result of close packing in the SAM, only minimal catalytic penetration and reduced reactivity takes place on such flat arrays in the absence of defects or terraces. With a monotonic increase in distance separating the metal support

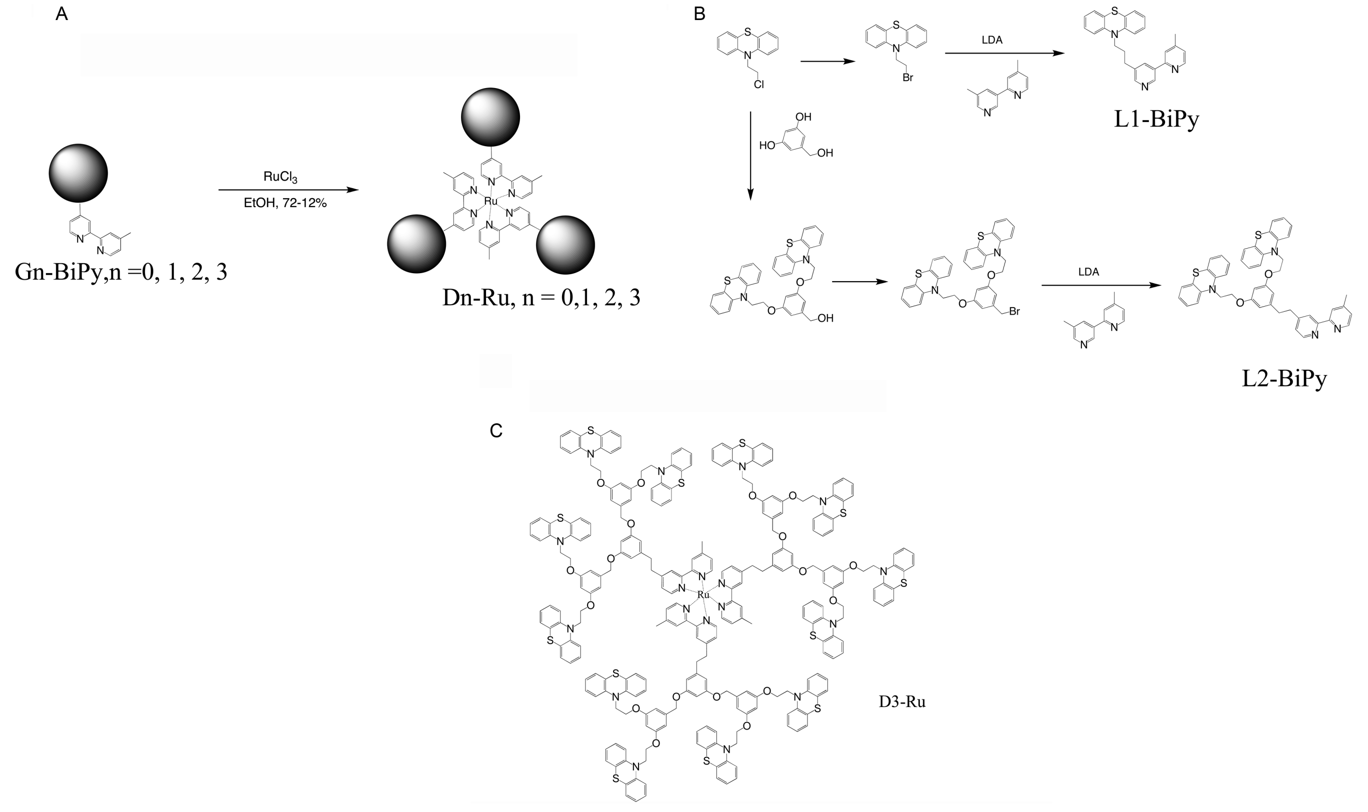

FIGURE 6. Dendrimer synthesis: (A) ligand prepared by metal coordination; (b) synthesis of first and second generation ligands; (c) third generation ligand.

and the external dye, a linear relationship develops between distance and fluorescence quenching, Figure 3a,b.

High density of photoactive groups can also be attained by attaching the dye of interest at the end of a bifunctional tether, which is anchored at the other end via a group with high chemical affinity for a metal or semiconductor surface. A common elaboration of this theme is encountered when an alkyl thiol is bound at the 1-position to a solid support and a dye of interest is appended to the *x* position, that is, HS-(CH2)*x*-dye. Fluorescence quenching proportional to the number of intervening methylene units shows that the linkers are densely packed but can effect through-bond electron transfer to multiple networked sites.

VIII. Shell–Core Clusters (SCCs)

Controlled charge migration can also be observed in clusters in which one spherical object completely surrounds another, the chemical composition of the two spheres being chemically different, Figure 4.

Van der Walls forces are responsible for the rapid formation of well-ordered arrays; that is, one that is insulating, and stable over time and space over distances that are large on a molecular scale. In Figure 5a, a semiconductor envelopes a defined metal cluster, whereas in Figure 4b a metal or metal complex caps the semiconductor nanoparticle.

As shown in Figure 5a, when connected to a gold surface through a thiol linkage, monolayer coverage produces a conformational rigidity cap. The outer coating is called a "shell" and the completely included inner sphere is called the "core". The migration of charge is typically accomplished as small neutral molecules or ions move, via random motion, to and across the shell–core interface, which is a close structural mimic of a tilted self-assembled monolayer (SAM). Indeed, included metal spheres around a micellar core envoke surface passivation as the basis for selective catalytic reactions dependent upon the selectivity of inhibition as the reactant passes through the surface-passivated dendrimeric shell.

Because of the versatility of possible synthetic routes to attain specific outer-shell functional shell–core nanoparticles, catalytic reactivity is directly affected by the chemical composition of both the inner and outer shells. Changes in the length between the central core and the outer shell, however, will reveal closer contacts, whether a SCC or a dendrimer D_x where *x* is the number of included dendrimeric generations, Figure 6a,b.

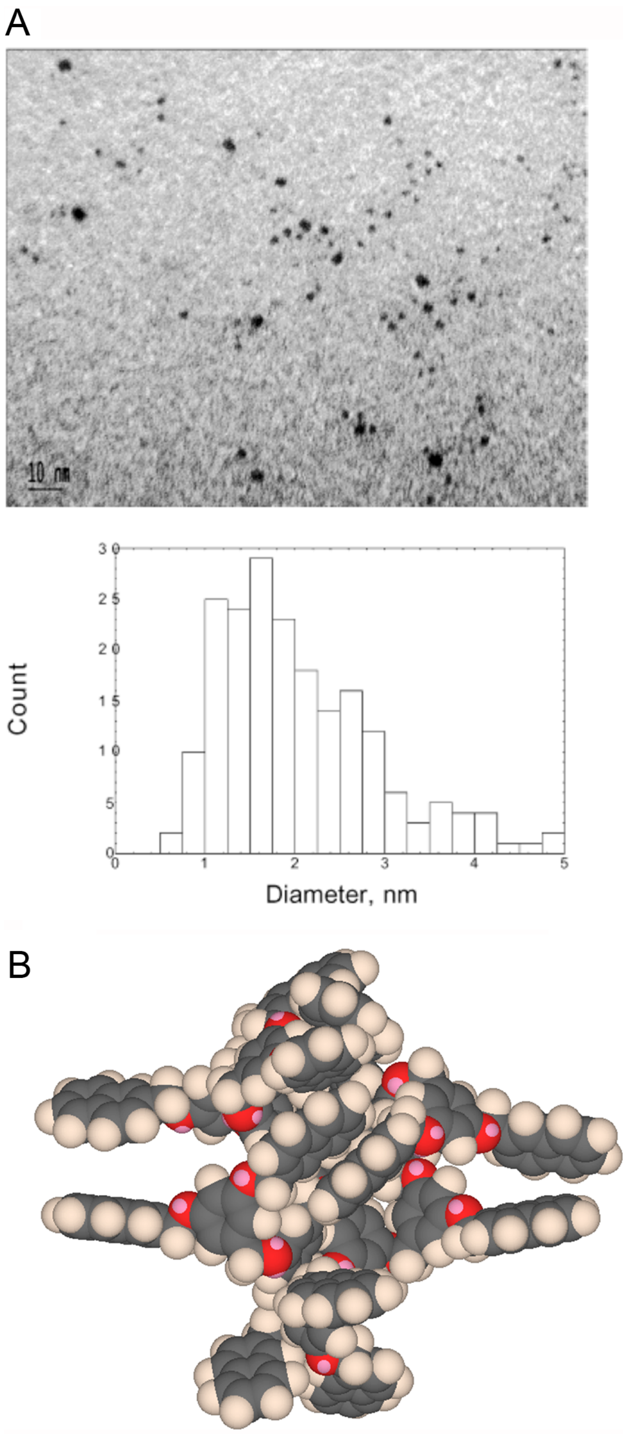

FIGURE 7. Structural characterization of Pd–third generation ligand complex: (a) TEM image and core-size histogram; (b) excimer formation in third generation dendrimer.

IX. Dendrimers

Roughly speaking, a dendrimer consists of a distinct core, which may or may not be photo- or electroactive, and several generations of appended branches. As a family, dendrimers may be produced via stepwise synthesis to achieve a defined size and hence a specific molecular weight. Synthetic approaches are either convergent or divergent, building successive generations through repeated employment of branched functionality from the core in a divergent synthesis and from the periphery in a convergent one. In either case, additional branching occurs as subsequent generations of ligated dyes are repeatedly added, Figure 7a–c.

Dendrimers are also well-defined spectroscopically and can be heavily loaded by covalently attaching a redox-active couple or a photoactive set of light absorbers. As each step of a dendrimer synthesis takes place, a bifunctional agent becomes available for extension of molecular weight in yet another step. In short, like the SSCs and the SAMs, dendrimers are highly organized and seem by some criteria to be biomimetic, especially in dealing with multiple charge events studied by pulse radiolysis.

A dendrimer has a branched terminus onto which multiple chromophores or redox reactants can be bound or adsorbed. They are also size-sensitive, and the molecular flexibility encountered in this series is accomplished by building multiple generations of these families. From such studies, we achieve an experimental definition of key reaction descriptors and discuss evidence about how local order influences the structure and reactivity of adsorbates small enough to be relevant to nanotechnology. In fact, micelles can be thought of as large SCCs, Figure 8a, which illustrates the use of transmission electron microscopy, core-size histograms and molecular mechanics calculations to characterize these arrays. The potential for multielectron accumulation is clear, Figure 8b.

The available chemical routes leading to SCCs, SAMs, and D*x* are normally sized at a molecular weight of a few thousand. If the chain length of the self-assembling branched unit is high, a nonhomogeneous micellar dispersion is formed. As shown in Figure 6, micelles can be obtained with trifunctional chains that lead to branching. Figure 6a shows micelle formation based upon metal coordination of a triply branched ligand, and Figure 6b shows the synthesis of first and second generation ligands. Similarly, Figure 6c shows a third generation ligand to be used in Figure 7b in the preparation of a third generation dendrimer.

Thus, high generations of dendrimers (greater than three generations), built upon covalent branching in the component starting materials, will physically resemble a self-assembled SCC or a micellar aggregate. The principal difference rests in the covalent construction of the dendrimer, which resists competitive hydrolysis in acidic or basic

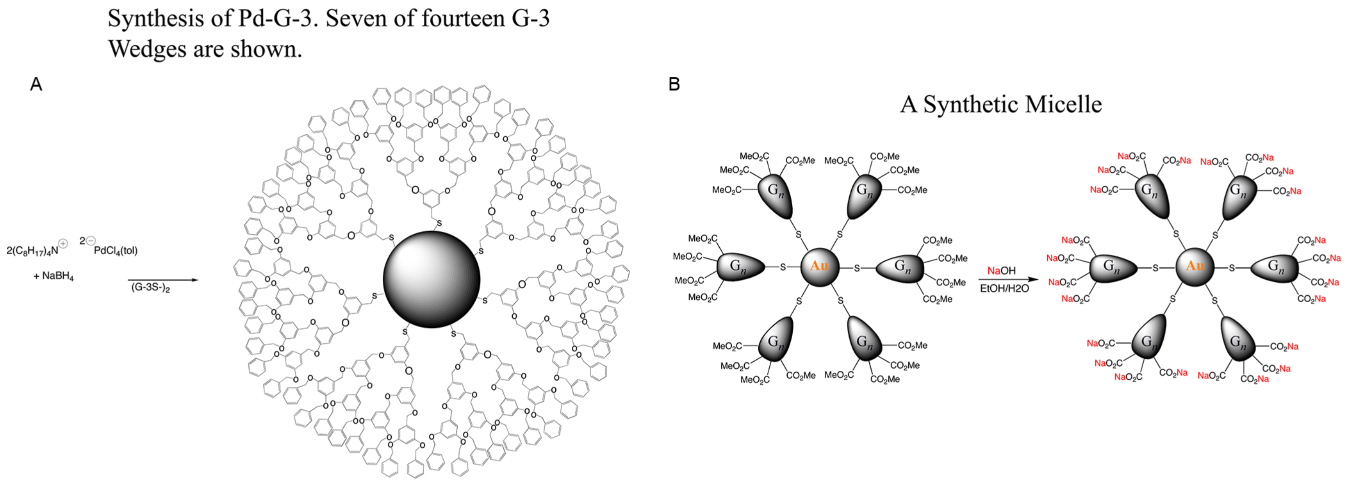

C Average physical parameters of Pd-G-3

Average core diameter	2.04nm
No. Pd Atoms in the core	302
No. of G-3 dendrons attached to Pd core	14
No. of atoms on the surface of Pd core	151*
Passivated Pd surface area	9%
Unpassivated Pd surface area	91%

*Assumes that 50% of atoms are on the surface for 2 nm Pd particle

FIGURE 8. Shell–core penetration for Pd catalytic coupling: (a) surface passivation by micelle shell; (b) catalytic turnover via micelle penetration by hydrolysis; (c) improved catalysis by passivated dendrimer.

media. In a micelle, in contrast, the outer shell is a neutral amide or ester group that is hydrolyzed to a multiple-site polyanion.

Surface charging upon basic hydrolysis is illustrated in Figure 8a,b. Here, are shown contrasting dendrimer structures possessing (a) metal coordination vs covalently bound cores and (b) micellar hydrolysis of a neutral aggregate. The dendrimeric shell can be modified by attachment of a highly absorptive and emissive dye of interest, either within the bifunctional monomer or after formation of a neutral micelle. As a result, structural characterization can be accomplished separately and by standard routes. Illustration of this structural preference involves (a) a core-size histogram and (b) calculated excimer formation in third-generation dendrimers. Shown in Figure 8a is an example of the structural characterization of a Pd–third-generation Ru complex.

Such complexes can be studied more easily than those derived from SAMs or SCCs, from an experimental or theoretical viewpoint. For example, Figure 8c shows that acceptable penetration into dendrimeric pores allows access to a Pd core for catalytic Heck coupling. And in fact, bonding between aryl halides and arenes is dramatically improved with a heavy metal core dendrimer as catalyst, both in significant rate enhancement and by a 10-fold improvement in catalytic turnover, Figure 8c.

Indeed, included metal nanoparticles as a micellar core look to surface passivation as the basis for selective catalytic reactions. Changes in the length and rigidity of the intervening tether between the central core and the outer shell will provide chemists with a new means of reaction control.

X. Conclusions

Structure–activity patterns based on improved and predictable utilization of self-assembled monolayers, shell–core clusters, and high generation dendrimers permit new routes for chemical control and new understanding of aggregation effects. These nonhomogeneous structures therefore represent an exciting new area for catalysis and photocatalysis. In exploring nonhomogeneous interactions, chemists will open a highly important route for controlling reactivity and for discovering multiple-photon and multiple-redox components in artificial photosynthesis. Active catalysts can provide new routes to steric inhibition, the first step toward selective access to the reactive surface, and in accumulation of active redox equivalents. In turn, these studies are likely to contribute to fundamental understanding of multiple electron transfer reactions in models that mimic the complex membrane-constrained events taking place during natural photosynthesis.

This work was supported by the Office of Basic Energy Sciences, Solar Photochemistry Division, of the United States Department of Energy.

BIOGRAPHICAL INFORMATION

Marye Anne Fox, a native of Canton, Ohio, received her undergraduate degree at Notre Dame College and her Ph.D. at Dartmouth College. After 32 years on the faculty of the University of Texas at Austin, she held June and Virgil Waggoner Regents Chair in Chemistry and served as Vice President for Research. She accepted the Chancellorship at North Carolina State University in 1998, and six years later was appointed Chancellor of the University of California, San Diego, from which she has recently returned to the faculty as a Distinguished Professor. She has received many important awards for teaching, mentoring, and research, including the National Medal of Science from President Obama. She and her husband are parents of five sons and grandparents of 10.

FOOTNOTES

The authors declare no competing financial interest.
Dedicated to Paul Barbara, who was a superb scientist and an even better friend.

REFERENCES

1 Sykora, M.; Maxwell, K. A.; DeSimone, J. M.; Meyer, T. J. Mimicking the antenna-electron transfer properties of photosynthesis. *Proc. Natl. Acad. Sci. U.S.A.* **2000**, *97*, 7682–7695.

2 Sundstrom, V.; Pullerits, T.; van Grondelle, R. Photosynthetic light-harvesting reconciling dynamics and structure of purple bacterial LH2 reveals function of photosynthetic array. *J. Phys. Chem B* **1999**, *103*, 2327–2346.

3 Montano, G. A.; Wu, H. M.; Lin, S.; Brune, D. C.; Blankenship, R. F. Isolation and Characterization of the B798 light-harvesting baseplate from the chlorosomes of *Chloroflexus aurantiacus*. *Biochemistry* **2003**, *42*, 10246–10251.

4 Watkins, D. M.; Fox, M. A. Rigid, well-defined block copolymers for efficient light harvesting. *J. Am. Chem. Soc.* **1994**, *116*, 644–662.

5 Watkins, D. M.; Fox, M. A. Light harvesting polymers. *Polym. Mater. Encycl.* **1996**, *5*, 3593–3597.

6 Stewart, G. M.; Fox, M. A. Chromophore-labeled dendrons as light harvesting antennae. *J. Am. Chem. Soc.* **1996**, *118*, 4354–4357.

7 Whitesell, J. K.; Chang, H. K.; Fox, M. A.; Galoppini, E.; Watkins, D. M.; Fox, H.; Hong, B. Anisotropic energy and electron migration in multichromophore-laden polymers on metal surfaces. *Pure Appl. Chem.* **1996**, *68*, 1469–1470.

8 Willemse, R. J.; Piet, J. J.; Warman, J. M.; Hartl, F.; Brouwer, A. M. Step-wise vs. direct long-range charge separation in molecular triads. *J. Am. Chem. Soc.* **2000**, *122*, 3721–3730.

9 Fox, M. A. Fundamentals in the design of molecular electronic devices: Long range charge carrier transport and electronic coupling. *Acc. Chem. Res.* **1999**, *32*, 201–210.

10 Kamat, P. V. Photophysical, photochemical, and photocatalytic aspects of metal nanoparticles. *J. Phys. Chem. B* **2002**, *106*, 7729–7752.

11 Love, J. C.; Wolfe, D. B.; Haash, R.; Chabinyc, M. L.; Paul, K. E.; Whitesides, G. M.; Nuzzo, R. G. Formation and structure of self-assembled monolayers of alkylthiolates on palladium. *J. Am. Chem. Soc.* **2003**, *125*, 1283–1322.

12 Pileni, M. P. Self-assembly of inorganic nanocrystals: Fabrication and collective intrinsic properties. *Acc. Chem. Res.* **2007**, *40*, 685–693.

13 Stupp, S. I.; LeBonheur, V.; Walker, K.; Li, L,S.; Huggins, K. E.; Keser, M.; Amstuzt, A. Supramolecular materials: Self-organized nanostructures. *Science* **1997**, *276*, 384–386.

14 Gu, T.; Whitesell, J. K.; Fox, M. A. Electrochemical charging of a fullerene-functionalized self-assembled monolayer on Au (111). *J. Org. Chem.* **2004**, *69*, 4075–4081.

15 Zhang, J.; Whitesell, J. K.; Fox, M. A. Photophysical behavior of pyrenyl probes of differently sized colloidal gold clusters capped with monolayers of an alkylstilbenethiolate. *J. Phys. Chem. B* **2003**, *107*, 6051–6057.

16 Hong, B.; Fox, M. A. Arene-functionalized polyisocyanides: Photophysics of well-defined homopolymers and block copolymers for efficient light harvesting. *Can. J. Chem.* **1995**, *73*, 2101–2107.

17 Chan, W. L.; Ligges, M.; Jailaubekov, A.; Kaake, L.; Avila, L. M.; Zhu, X. Y. Observing the multiexciton state in singlet fission and ensuing ultrafast multi-electron transfer. *Science* **2011**, *334*, 1541–1553.

18 Hu, J.; Liu, F.; Zhang, J.; Whitesell, J. K.; Fox, M. A. Competitive photochemical activity in a self-assembled monolayer on a colloidal gold cluster. *J. Am. Chem. Soc.* **2001**, *123*, 14664–14675.

19 Kittredge, K.; Fox, M. A.; Whitesell, J. K. Helical polypeptide films grown from thiol linkers on gold surfaces. *Helv. Chim. Acta* **2002**, *85*, 768–775.

20 Zhang, J.; Whuitesell, J. K.; Fox, M. A. Photoreactivity of self-assembled monolayers of azobenzene or stilbene derivatives capped on colloidal gold clusters. *Chem. Mater.* **2001**, *13*, 2323–2348.

21 Kittredge, K.; Whitesell, J. K.; Fox, M. A. Effect of the alkyl chain length on the fluorescence of 9-alkylfluorenyl thiols as self-assembled monolayers on gold. *J. Phys. Chem. B* **2001**, *105*, 10594–10599.

22 Reese, R. S.; Fox, M. A. Self-assembled monolayers on gold of thiols incorporating conjugated terminal groups. *J. Phys. Chem.* **1998**, *102*, 9820–9845.

23 (a) Zhou, J.; Sedev, R.; Beattie, D.; Ralston, J. Light-induced aggregation of colloidal gold nanoparticles capped by thymine derivatives. *Langmuir* **2008**, *254*, 4506–4511. (b) Zhou, J.; Sedev, R.; Beattie, D.; Ralston, J. Synthesis and surface structure of thymine-functioinalized self-assembled monolayer-protected gold nanoparticles. *Langmuir* **2007**, *23*, 9170–9178.

24 Hoener, C. F.; Allan, K. A.; Bard, A. J.; Campion, A.; Fox, M. A.; Mallouk, T. E.; Webber, S. E.; White, J. M. Demonstration of a shell-core structure in layered CdSe−ZnSe small particles by X-ray photoelectron and Auger spectroscopies. *J. Phys. Chem.* **1992**, *96*, 3812–3817.

25 Canepa, M.; Fox, M. A.; Whitesell, J. K. The influence of core size on electronic coupling in shell-core nanoparticles: Gold clusters capped by pyrenoxylalkylthiolate. *Photochem. Photobiol. Sci.* **2003**, *2*, 1177–1183.

26 Zahavy, E.; Whitesell, J. K.; Fox, M. A. Surface effects in water-soluble shell−core hybrid gold nanoparticles in oligonucleotide single strand recognition for sequence-specific bioactivation. *Langmuir* **2010**, *26*, 16442–16446.

27 Nerambourg, N.; Wertz, M. H. V.; Charlot, M.; Blanchard-Desce, M. Quenching of molecular fluorescence on the surface of monolayer-protected gold nanoparticles investigated using place exchange equilibria. *Langmuir* **2007**, *23*, 5563–5570.

28 Tam, J. M.; Murthy, A. K.; Ingram, D. R.; Nguyen, R.; Sokolov, K. V.; Johnston, K. P. Kinetic assembly of near-IR-active gold nanoclusters using weakly adsorbing polymers to control size. *Langmuir* **2010**, *26*, 8988–8999.

29 Fossom, R. D.; Fox, M. A. Dual exciplex formation and photoinduced electron transfer in pyrene end-labeled polynorbornenes. *J. Phys. Chem. B* **1997**, *101*, 2526–2550.

30 Watkins, D. M.; Fox, M. A. Photoinduced charge separation and photophysical dynamics in polynorbornene chromophore-labeled and quencher-labeled block copolymers. *J. Am. Chem. Soc.* **1996**, *118*, 4344–4354.

31 Fox, M. A.; Thompson, H. W. Synthesis and photophysical characterization of group transfer polymers with pendent aryl chromophores. *Macromolecules* **1997**, *30*, 7391–7403.

32 Fossum, R. D.; Fox, M. A. Photoinduced electron transfer in pyrene-labeled polynorbornenes. *Polym. Mater. Sci. Eng.* **1997**, *76*, 389–397.

33 Watkins, D. M.; Fox, M. A. Photoinduced charge separation and photophysical dynamics in polynorbornene chromophore-labeled and quencher-labeled block copolymers. *J. Am. Chem. Soc.* **1996**, *118*, 4344–4357.

34 Rusa, M.; Whitesell, J. K.; Fox, M. A. Controlled fabrication of gold/polymer nanocomposites with a highly structured poly(N-acylethyleneimine) shell. *Macromolecules* **2004**, *37*, 2766–2778.

35 Fossum, R. D.; Fox, M. A. Dual exciplex formation and photoinduced electron transfer in pyrene-labeled polynorbornenes. *Polym. Mater. Sci. Eng.* **1997**, *101*, 2526–2543.

36 Fossum, R. D.; Fox, M. A. Intramolecular complex formation and triplet energy transfer in polynorbornenes incorporating benzophenone. *J. Am. Chem. Soc.* **1997**, *119*, 1197–1226.

37 Santos, M.; Fox, M. A. Hydrogen bonding interactions between starburst dendrimers and several molecules of biological interest. *J. Phys. Org. Chem.* **1999**, *12*, 293–298.

38 Zhu, L.; Magde, D.; Whitesell, J. K.; Fox, M. A. Optical and electrochemical properties of shell-core dendrimers: Ruthenium coordination complexes capped with a range of sized phenothiazine-substituted bipyridines. *Inorg. Chem.* **2009**, *48*, 1811–1818.

39 Ghaddar, T. H.; Wishart, J. F.; Thompson, D. W.; Whitesell, J. K.; Fox, M. A. A dendrimer-based electron antenna: Paired electron transfer reactions in dendrimers with a 4,4′-bipyridine core and multiple naphthalene peripheral groups. *J. Am. Chem. Soc.* **2002**, *124*, 8285–8299.

40 Ghaddar, T. H.; Wishart, J. F.; Kirby, J. P.; Whitesell, J. K.; Fox, M. A. Pulse radiolysis studies of dendritic macromolecules with biphenyl peripheral groups and a ruthenium tris-bipyridine core. *J. Am. Chem. Soc.* **2001**, *123*, 12832–12839.

41 Cho, T. J.; Zangmeister, R. A.; MacCuspie, R. I.; Patru, A. K.; Hackley, V. A. Newkome-type dendron-stabilized gold nanoparticles: Synthesis, reactivity, and stability. *Chem. Mater.* **2011**, *35*, 3446–3449.

42 Gu, T.; Ye, T.; Simon, J. D.; Whitesell, J. K. Subpicosecond transient dynamics in gold nanoparticles encapsulated by a fluorophore-terminated monolayer. *J. Phys. Chem. B* **2003**, *107*, 1765–1780.

43 Gopidas, K. R.; Whitesell, J. K.; Fox, M. A. Metal core−organic shell dendrimers as unimolecular micelles. *J. Am. Chem. Soc.* **2003**, *125*, 14168–14180.

44 Ghaddar, T. H.; Whitesell, J. K.; Fox, M. A. Excimer formation in a naphthalene-labeled dendrimer. *J. Phys. Chem. B* **2001**, *105*, 8729–8735.

45 Gu, T.; Whitesell, J. K.; Fox, M. A. Intramolecular charge transfer in a 1:1 Cu(II)/prenylcyclam dendrimer complexes. *J. Phys. Chem.* **2006**, *110*, 25149–25152.

46 Stewart, G. M.; Fox, M. A. Dendrimer-linear polymer hybrids through ROMP. *Chem. Mater.* **1998**, *10*, 860–863.

47 Gopidas, K. V.; Whitesell, J. K.; Fox, M. A. Nanoparticle-cored dendrimers: Synthesis and characterization. *J. Am. Chem. Soc.* **2003**, *125*, 6491–6498.

48 Hu, J.; Liu, F.; Zhang, J.; Kittredge, K.; Fox, M. A.; Whitesell, J. K. Competitive photochemical reactivity in a self-assembled monolayer on a colloidal gold cluster. *J. Am. Chem. Soc.* **2001**, *123*, 1464–1474.

49 Peng, Z.; Walther, T.; Kleinermanns, K. Photofragmentation of phase-transferred gold nanoparticles by intense pulsed laser light. *J. Phys. Chem. B* **2005**, *109*, 15735–15740.

50 Lee, Y. J.; Zhang, T.; Barbara, P. F. Kinetics of electron attachment to reverse micelles. *J. Phys. Chem. B* **2004**, *108*, 5175–5178.

51 Liu, C. Y.; Pan, H. L.; Fox, M. A.; Bard, A. J. Reversible charge trapping/detrapping in a photoconductive /insulator of liquid crystal zinc porphyrin. *Chem. Mater.* **1997**, *9*, 1422–1430.

52 BoubbouK. , H.; Ghaddar, T. H. Electrostatic layer-by-layer deposition of photoactive dendrimers with tri-viologen-like cores on their surfaces: Synthesis and electrochemical and photocurrent generation measurements. *Langmuir* **2005**, *21*, 8844–8851.

53 Howell, A. R.; Fox, M. A. Steady state fluorescence of dye-sensitized TiO_2 xerogels and aerogels as a probe for local chromophore aggregation. *J. Phys. Chem. A* **2003**, *107*, 3300–3304.

54 Andreasson, J.; Pischel, U; Straight, S. D.; Moore, T. A.; Moore, A. L.; Gust, D. All-photonic multifunctional molecular logic devices. *Proc. Natl. Acad. Sci. U.S.A.* **2011**, *108*, 6532–6543.

55 Ghorai, K.;G.; Glotzer, S. C. Atomistic simulation of striped phase separation in mixed-ligand self-assembled monolayer-coated particles. *J. Phys. Chem. C* **2010**, *114*, 19182–19197.

56 Prieto, I.; Teetsov, J.; Fox, M. A.; vandenBout, D. A.; Bard, A. J. A study of excimer emission in solutions of (poly-dioctylfluorene) using electrogenerated chemiluminscence. *J. Phys. Chem. A* **2001**, *105*, 520–524.

57 Saunders, A. E.; Ghezelbash, D. M.; Stowell, C. A.; Korgel, B. A. Columnar self- assembly of colloidal nanodisks. *Nano Lett.* **2006**, *6*, 2959–2963.

58 Alahann, J.; Somorjai, G.; A.; Langer, B. A reversibly switching surface. *Science* **2003**, 371–376.

59 Gur, I.; Fromer, N. A.; Geier, M. L.; Alivasatos, A. P. Air-stable all-inorganic nanocrystal solar cells processed from solution. *Science* **2005**, *310*, 462–466.